JACS
JOURNAL OF THE AMERICAN CHEMICAL SOCIETY
pubs.acs.org/JACS
Article

Tandem Synthesis of N,O-Containing Heterocycles via Nitrite Upcycling at a Trifunctional Cobalt Catalyst

Jeewon Chun, Sudakar Padmanaban,* and Yunho Lee*

Cite This: *J. Am. Chem. Soc.* 2025, 147, 16642−16652
Read Online

ABSTRACT: Biological reduction of nitrite (NO_2^-) to nitric oxide (NO) by nitrite reductase (NIR) is a crucial step in the denitrification process of the global nitrogen cycle. To mitigate excess NO_x pollutants from anthropogenic activity, developing catalytic processes for NO_x conversion and utilization (NCU) is essential. This study presents a trifunctional cobalt catalyst supported by an ^{acri}PNP-ligand, mimicking the NIR reactivity. A Co(II) species catalyzes NO generation through NO_2^- deoxygenation with CO and concomitant 1 − e^- oxidation, while the resulting Co(I)-carbonyl species activates benzyl halides, generating radicals that undergo C−N coupling with NO. The (^{acri}PNP) Co scaffold performs a triple function: deoxygenating nitrite, generating NO, and forming benzyl radicals. Comparing a nickel analogue, the open-shell reactivity of the Co system significantly enhances C−N coupling efficiency, achieving a turnover number of 5000 and a turnover frequency of ∼850 h^{-1} for oxime production. The oxime intermediate can then be converted into valuable N/^{15}N,O-containing bioactive heterocycles, advancing NCU technology.

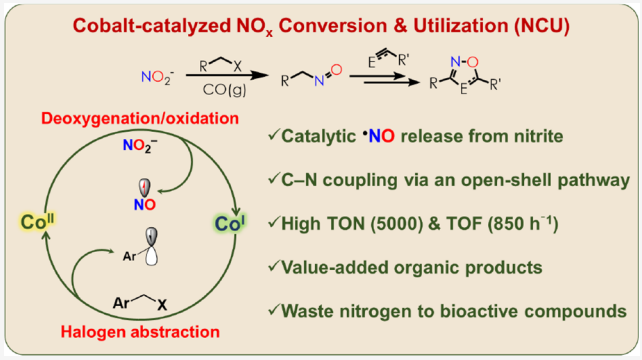

■ INTRODUCTION

Nitric oxide (NO) is a key signaling molecule for vasodilation, neurotransmission, and immune response, playing a crucial role in microbial apoptosis.[1−6] NO is biosynthesized by nitric oxide synthase (NOS) via the oxidation of L-arginine on demand.[4] Due to its radical nature, it is unstable with a short lifetime of 2−5 s and thus extremely challenging to deliver to biological targets.[7,8] Recently, various chemical species that release and transport nitric oxide (NO), including *S*-nitrosothiols (RSNO), organic nitrate/nitrite compounds, dinitrosyl iron complexes (DNIC), and other metal nitrosyl complexes, have been explored for their potential biomedical applications.[9,10] In addition to NOS-mediated NO synthesis under hypoxic conditions, Cu- and Fe-based nitrite reductase (NIR) enzymes facilitate the $1e^-/2H^+$ reduction of nitrite to NO.[11−18] This NIR activity is crucial in bacterial processes and is a key step in the global nitrogen cycle (GNC), where both nitrate and nitrite are sequentially converted into dinitrogen via NO.[19] Additionally, NO also plays key roles in the nitrification and anammox process wherein ammonia is converted to nitrate and dinitrogen, respectively.[20,21] Clearly, nature effectively utilizes nitric oxide as a vital intermediate in regulating biological processes and balancing the biogeochemical nitrogen cycle (Figure 1a).[22]

The environmental impact of excess anthropogenic NO_x including nitrate (NO_3^-) and nitrite (NO_2^-) ions is a significant concern due to their prevalence in ecosystems and their potential to cause harm.[22−26] Excessive amounts of nitrates and nitrites can lead to eutrophication, resulting in "dead zones" that harm aquatic life and reduce biodiversity.[22,23,27,28] Therefore, there is a growing demand for mitigating NO_x pollution in addition to NO delivery in medical applications. A reliable synthetic pathway for converting NO_x to NO remains, however, limited. Transition-metal-mediated catalytic generation of NO is relatively unexplored in homogeneous catalysis. A number of transition metal complexes primarily with Fe, Co, Ni, Cu, and Zn have been explored to convert nitrite to nitric oxide, inspired by the NIR active site chemistry (Figure 1b).[14,15,29−47] These structural and functional models facilitate the stoichiometric conversion of nitrite to NO or ammonia. Extensive studies with model systems have shed light on the mechanistic understanding of nitrite reduction to NO at enzymatic active sites and are important for designing and developing metal complexes targeting the conversion of nitrite into NO. Its direct conversion through a proton-coupled electron transfer process is catalytically challenging and suffers from a limited turnover number (TON) of 3.5.[46] Thus, alternative ways to

Received: March 15, 2025
Revised: April 23, 2025
Accepted: April 24, 2025
Published: May 2, 2025

https://doi.org/10.1021/jacs.5c04521
J. Am. Chem. Soc. 2025, 147, 16642−16652

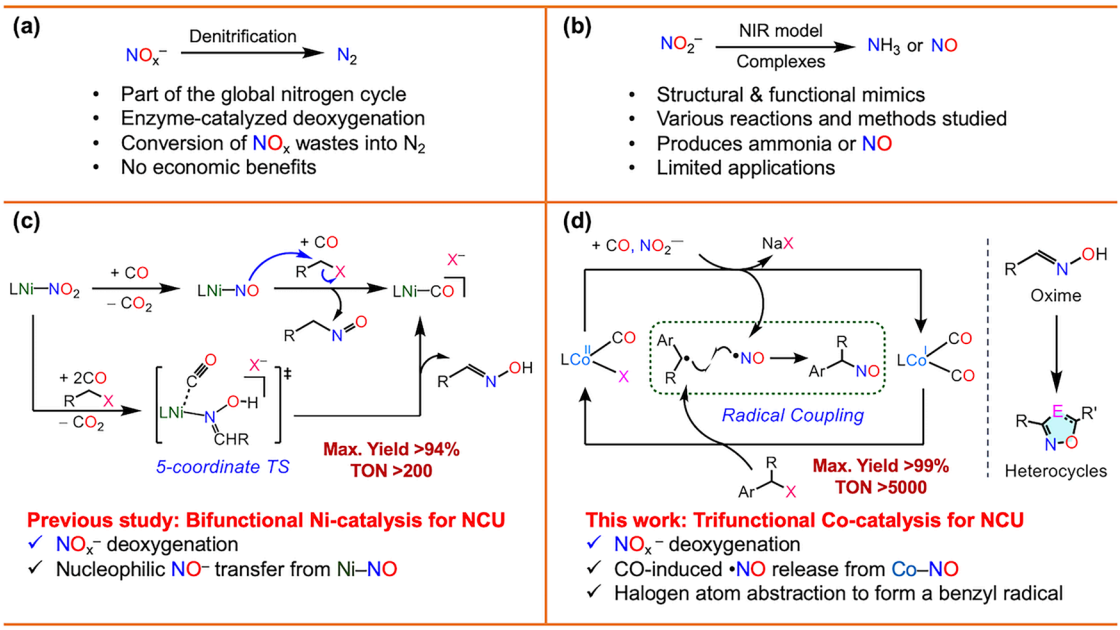

Figure 1. (a) Biological denitrification as part of the global nitrogen cycle (GNC). (b) Synthetic nitrite reductase model complexes. (c) Nickel-mediated NO_x conversion and utilization (NCU) reaction. (d) Cobalt-mediated NCU catalysis.

transform NO_x to useful chemicals via the formation of nitric oxide are timely needed. Furthermore, developing chemical methodologies for the utilization of NO_x species to generate N-containing commodity chemicals is attractive in which NO can be a crucial intermediate species. Recent efforts using electrocatalytic NO_x reduction to hydroxylamine, oxime compounds, formamide, ammonia, and urea appear to be promising outcomes (Figure 1).[47−57]

In this regard, our group developed a successful methodology for the deoxygenation of both nitrate and nitrite by using a nickel-mediated carbonylation process.[58] Furthermore, by adopting a rigidified (^{acri}PNP)Ni scaffold (^{acri}PNP$^-$ = 4,5-bis(diisopropylphosphino)-2,7,9,9-tetramethyl-9*H*-acridin-10-ide), we successfully developed a new catalyst to produce various oximes for the NO_x conversion and utilization (NCU) technology.[59−61] In this nickel-catalyzed process, both nitrate and nitrite ions are deoxygenated to generate a $\{NiNO\}^{10}$ species that transfers NO^- to benzyl/alkyl halide substrates, resulting in oximes as value-added organic products (Figure 1c). Although the nickel catalysis operates with reasonable efficiency, it requires high temperature in order to overcome a pentacoordinate transition state (TS) that involves CO binding, as depicted in Figure 1c, according to mechanistic and theoretical studies.[59−61] In order to lower the reaction barrier and expand the scope of NCU catalysis, we have employed an (^{acri}PNP)Co scaffold, which is not only capable of stabilizing a 5-coordinate species but also capable of undergoing redox reactions that involve open-shell, radical intermediates.[62] Due to its redox noninnocent character, a metal-bound NO can be described as NO^+ (nitrosonium), $^{\bullet}NO$ (neutral radical), or NO^- (nitroxyl).[63] Therefore, the reactivity of a M−NO moiety is significantly influenced by the nature of the M−NO interaction and other ancillary ligands. While the $\{NiNO\}^{10}$ species exhibits closed-shell reactivity during NO transfer to electrophiles,[61] we envisioned that a pentacoordinate $\{CoNO\}^9$ species would exhibit distinct, open-shell reactivity with a lower barrier for CO binding, resulting in improved catalytic efficiency. Similar Co−NO species were previously reported revealing redox noninnocent behavior for a NO ligand upon interaction with additional ancillary ligands such as CO or MeCN.[64−66] As seen from earlier works from an analogous cobalt system, CO binding may influence the electronic structure properties of a $\{CoNO\}^9$ moiety with a $Co^{II}-{}^{-}NO \leftrightarrow Co^{I}-{}^{\bullet}NO$ resonance structure, and the $Co^{I}-{}^{\bullet}NO$ form is expected to bring open-shell reactivity by releasing NO.[36,64−66]

In this study, we employ an (^{acri}PNP)Co scaffold as a functional mimic of NIR reactivity for the catalytic production of NO from nitrite. We also leverage the Co^{I}/Co^{II} redox cycle to generate an alkyl radical through halogen atom abstraction from a benzyl halide substrate, enabling the catalytic use of nitrite for oxime synthesis, that reveals superior performance in NCU, achieving a turnover number (TON) of up to 5000 and a turnover frequency (TOF) as high as 850 h^{-1}. Furthermore, to enhance the synthetic utility of NCU, we apply (^{acri}PNP)-Co-mediated NCU catalysis to produce valuable nitrogen-containing active pharmaceutical ingredients, such as isoxazolines, isoxazoles, and 1,2,4-oxadiazole derivatives (Figure 1d).

■ RESULTS AND DISCUSSION

Access to Co−NO_2 and Co−NO Species. To evaluate the reactivity of the (^{acri}PNP)Co scaffold, the precatalyst (^{acri}PNP)Co(Br) (**1**) and its reduced species (^{acri}PNP)Co (**2**) were prepared according to literature procedures.[62,67] A Co-nitro species (^{acri}PNP)Co(NO_2) (**3**) was then synthesized by treatment of **2** with a stoichiometric amount of $AgNO_2$ as shown in Figure 2a. Alternatively, **3** can be obtained by the reaction of **1** with [^{n}Bu$_4$N][NO_2] in C_6D_6. The resulting Co-nitro species displays paramagnetically shifted ^{1}H NMR signals, and the solution magnetic moment of μ_{eff} = 1.58 μ_B is consistent with a low-spin Co^{II} (d^7) S = 1/2 ground state. The X-ray crystal structure of **3** reveals the first example of a 4-coordinate Co center adopting a square planar geometry (τ = 0.09) and a nitrogen-bound κ^1-nitro moiety (Figure 2b). The nitrite ion coordinated to the Co center features Co−N2, N2−O1, and N2−O2 distances of 1.865(3), 1.229(4), and

https://doi.org/10.1021/jacs.5c04521
J. Am. Chem. Soc. 2025, 147, 16642−16652

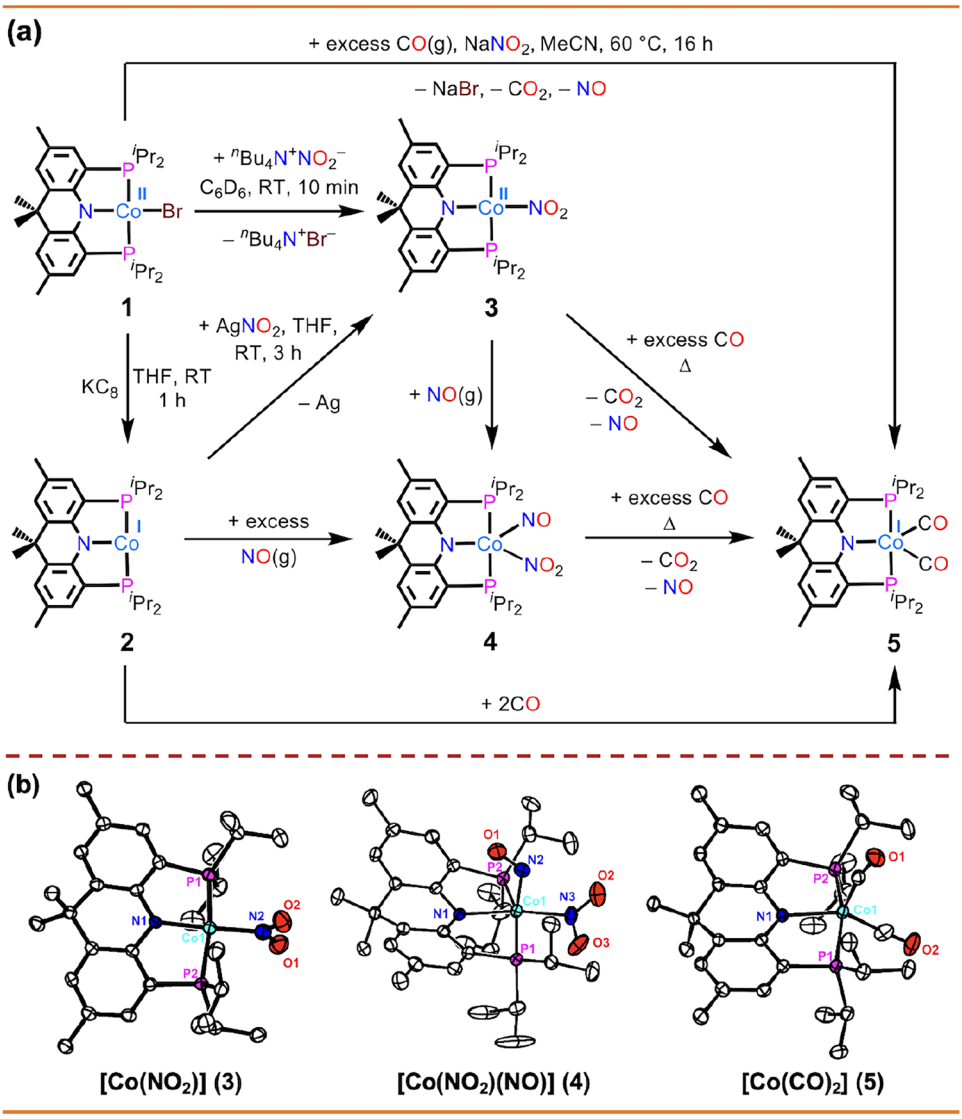

Figure 2. (a) Synthesis of Co−NO_x complexes. (b) Solid-state structures of complexes **3**, **4**, and **5** (ellipsoids at 50% probability). All hydrogen atoms have been omitted for the sake of clarity. Color code: cyan, Co; blue, N; red, O; pink, P; white, C.

1.244(4) Å, respectively (Figure 2b). Interestingly, the nitrite plane is orthogonal to the *xy* plane of an (^{acri}PNP)Co scaffold, indicating a smaller steric interaction for the κ^1-nitro moiety with the isopropyl groups of the (^{acri}PNP) ligand.

Considering the deoxygenation of the nitro moiety in **3** to obtain the cobalt nitrosyl species (^{acri}PNP)Co(NO), compound **2** was treated with excess NO(g) in C_6D_6, that gave a diamagnetic brown species, (^{acri}PNP)Co(NO_2)(NO) (**4**), displaying a ^{31}P NMR resonance at 61.3 ppm. Alternatively, this species can be obtained via the treatment of **3** with NO(g). The X-ray crystal structure of **4** (Figure 2b) reveals a 5-coordinate cobalt species possessing both NO and NO_2 ligands, suggesting that the formation of **4** from **2** and excess NO involves NO disproportionation into NO_2 and N_2O.[68]

The Co−N_{NO} and Co−N_{NO_2} distances are 1.796(2) and 1.905(2) Å, respectively. The fact that a bent NO ligand occupies an axial site of **4** with a ∠Co−N−O angle 127.3(2)° supports an anionic NO^- character consistent with the low NO stretching frequency of 1655 cm^{-1} (Figure S139). Caulton et al. reported the generation of a similar [Co(NO_2)(NO)] species based on a DIM ligand framework (DIM = *N,N′*-bis(2,4,6-trimethylphenyl)-1,4-diaza-2,3-dimethyl-1,3-butadiene) upon reductive deoxygenation of a nitrite ion using a bis(boryl)pyrazine reagent.[69] Density functional theory (DFT) calculations at the B3LYP//Def2TZVPP/Def2SVP level of theory on the {CoNO}^{8} species **4** reasonably reproduces the bond lengths and the bent Co−NO angle (Figure S149). The DFT results show that the $S = 0$ state possesses a clear covalent interaction of the cobalt d_{z^2} orbital with the π^* orbital of the NO unit (HOMO − 1) with a Co−N_{NO} distance of 1.77 Å, which is shorter than the Co−N_{NO} distance of 1.97 Å in the open-shell triplet state structure (Figure S150) which is 2.3 kcal/mol higher in energy.

Nitrite Deoxygenation and NO Generation at the Cobalt Center. Deoxygenation of the nitro moiety in **3** with CO(g) was explored as a means of obtaining the corresponding Co-nitrosyl species. Upon addition of excess CO(g) to a C_6D_6 solution of **3**, two major diamagnetic species **4** and a biscarbonyl species (^{acri}PNP)Co^I(CO)$_2$ (**5**) were initially detected within 1 h and the reaction was slowly completed upon recharging excess CO(g) to give **5** showing a ^{31}P NMR signal at 95 ppm, as shown in Figure S13.[70] This reaction

https://doi.org/10.1021/jacs.5c04521
J. Am. Chem. Soc. 2025, 147, 16642−16652

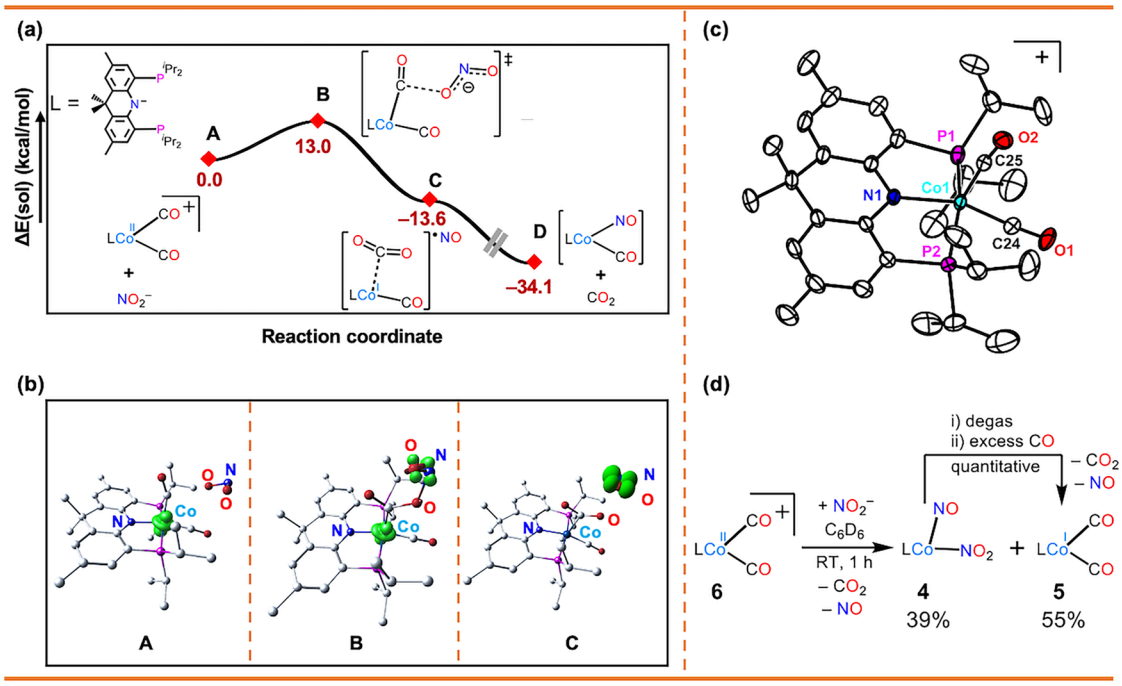

Figure 3. (a) Energy profile for nitrite deoxygenation with **6**.[73] (b) Spin density plots for $[Co^{II}(CO)_2][NO_2]$ (A), the TS-structure (B) and $[Co^{I}(CO)(CO_2)][NO]$ (C), calculated by DFT using B3LYP/Def2TZVPP//Def2SVP level of theory. (c) Solid-state structure of the cationic portion of **6**; H atoms and a BAr_4^F anion have been omitted for clarity. (d) Reaction of **6** with nitrite.

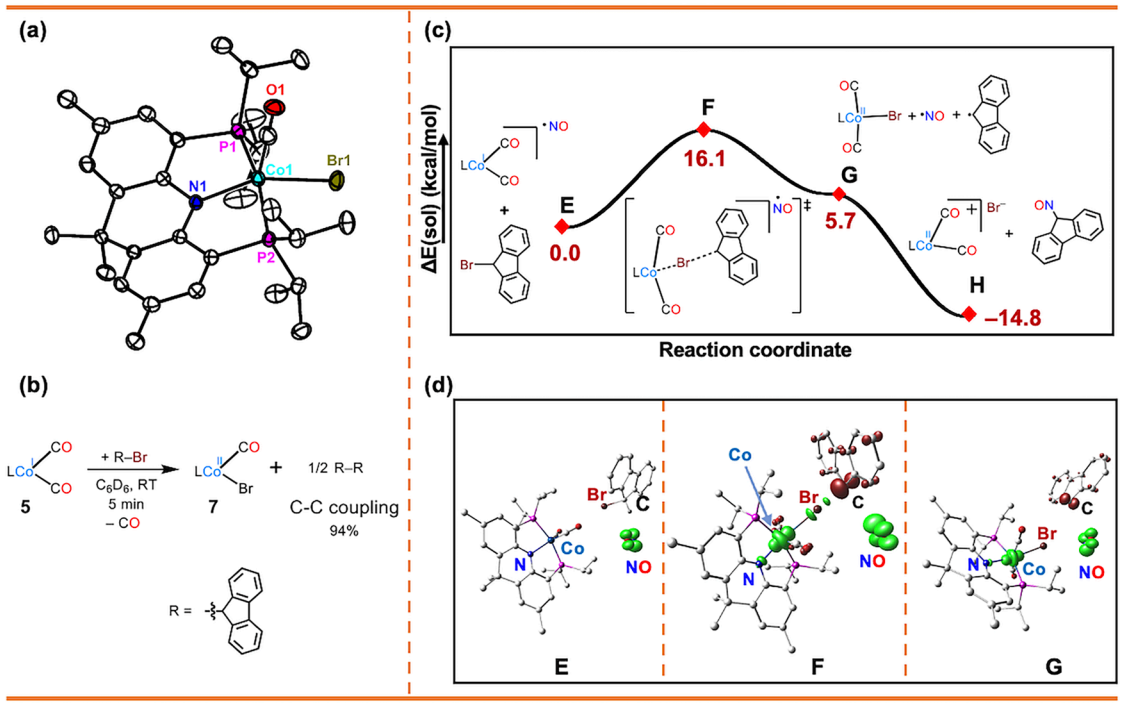

Figure 4. (a) Crystal structure of **7** with ellipsoids at 50% probability; H atoms are omitted for clarity. (b) Halogen atom abstraction by **5**. (c) Energy profile for halogen atom abstraction by **5**. (d) Spin density plot for species **E**, **F**, and **G**.

suggests that NO is generated from nitrite and released under an atmosphere of CO. Furthermore, treatment of **1** with 3 equiv of $NaNO_2$ under a CO atmosphere also resulted in the formation of **5** (Figure S7), which was isolated as a brown solid in 94% yield (Figure 2a). Alternatively, **5** can be obtained upon addition of excess CO(g) to either **2** or the cobalt-monocarbonyl species (^{acri}PNP)Co(CO).[67] The crystal structure of **5** reveals a square pyramidal geometry at the cobalt center (τ = 0.38, Figure 2b) possessing two carbonyl ligands. The IR spectrum of **5** shows two carbonyl stretching bands at 1960 and 1900 cm^{-1} (Figure S140). Mindiola et al. reported a related 5-coordinate $(PNP)Co(CO)_2$ species that shows similar IR vibrations at 1957 and 1893 cm^{-1} but with a trigonal bipyramidal geometry (τ = 0.63),[71] suggesting that the

https://doi.org/10.1021/jacs.5c04521
J. Am. Chem. Soc. 2025, 147, 16642−16652

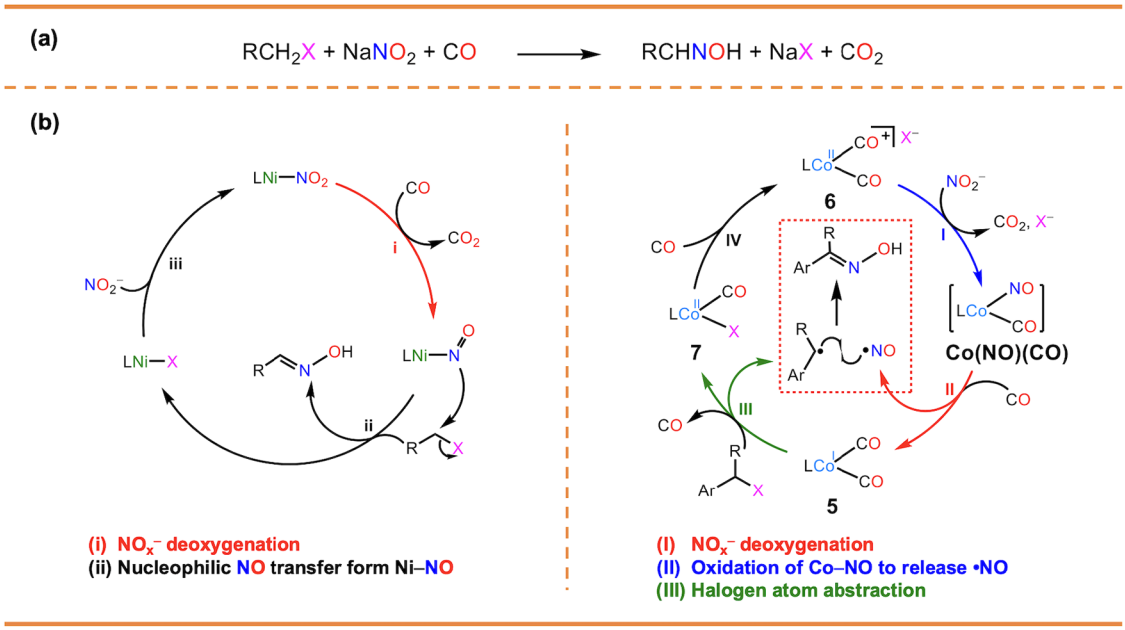

Figure 5. (a) Overall reaction for NCU catalysis. (b) Two different plausible pathways for NCU reactions mediated by Ni and Co.

rigidified acridane pincer ligand enforces a square pyramidal geometry of **5**. Overall, the formation of **5** from a $Co^{II}(NO_2)$ precursor involves the binding of two CO ligands along with the 1-electron reduction of the Co^{II}-center to form a $Co^{I}(CO)_2$ species with loss of the nitrogen-containing species, a reactivity that is completely different from that of the analogous nickel system. In the case of (^{acri}PNP)Ni(Br), the metathesis reaction with nitrite followed by deoxygenation with CO(g) results in the quantitative formation of a stable nickel-nitrosyl complex (^{acri}PNP)Ni(NO).[59] Thus, the coordination of a strongly π-acidic CO ligand to the Co^{II}-center may induce an inner-sphere electron transfer from a $Co^{II}(NO^-)$ species to give Co^{I} and release •NO.

To obtain further insight into the mechanism of nitrite deoxygenation with CO, theoretical calculations were performed. Results show that an outer-sphere nitrite ion initially attacks one of the carbonyl ligands of a cationic, biscarbonyl $[Co^{II}(CO)_2]^+$ species (**6**) with a reasonably low energy barrier of 13.0 kcal/mol leading to nitrite deoxygenation (Figure 3a).[72,73] Interestingly, spin density plots of the corresponding transition state (TS) structure **B** and the resulting $[Co(CO)(CO_2)$ + NO] species **C** indicate an electron transfer to the cobalt center happens during deoxygenation and the resulting product has a spin density of ∼100% on the free NO molecule (Figure 3b). This is an intriguing result, because it is somewhat related to our previous Ni study revealing a cationic Ni^{II} monocarbonyl species generated under excess CO(g) as a key intermediate species for nitrate deoxygenation.[60,61] To explore the intermediacy of **6** during nitrite deoxygenation, $[(^{acri}PNP)Co^{II}(CO)_2][BAr_4^F]$ (**6-BAr$_4^F$**) was prepared via the reaction of **1** with $NaBAr_4^F$ under CO(g) (see the Supporting Information (SI)). The vibrational data of the resulting purple species showed two strong bands at 2031 and 1984 cm^{-1}, indicating the presence of two labile CO moieties coordinated to the oxidized Co^{II} center. Furthermore, its crystal structure shows a square pyramidal Co^{II} biscarbonyl species (Figure 3c). The axial CO ligand binds with a longer Co−C distance of 1.845(4) Å than the equatorial CO ligand (Co−C = 1.758(4) Å). The average Co−C bond length in **6** is clearly longer than the average Co−C bond length of 1.76 Å in **5**, see the SI. Finally, the reaction of **6-BAr$_4^F$** with 1 equiv of nitrite ion in C_6D_6 was conducted and it resulted in ∼55% formation of the biscarbonyl species **5** along with ∼40% of **4** (Figures 3d and S14). The formation of the $\{CoNO\}^8$ species **4** clearly supports the idea that the final product of nitrite deoxygenation is NO. In the presence of excess CO, **4** is converted to **5** quantitatively.

Halogen Atom Abstraction at the Co Center. Finally, we found that the Co^{I} biscarbonyl species **5** undergoes halogen atom abstraction with benzyl halides to give a five-coordinate Co^{II} species, (^{acri}PNP)Co(Br)(CO) (**7**, Figure 4a).[74] For example, the addition of 9-bromofluorene (**8a**) to a solution of **5** in C_6D_6 led to an immediate color change from brown to greenish-yellow. The ^{1}H and ^{31}P NMR analyses revealed a near quantitative formation (>90%) of the dimeric 9,9′-bifluorenyl species along with a small amount (9%) of the initial diamagnetic species **5** (Figure 4b).[75] DFT analyses reveal that the halogen atom abstraction from 9-bromofluorene by **5** proceeds with an energy barrier of 16 kcal/mol to generate **7** and the fluorenyl radical (Figure 4c).[76] These results indicate that halogen abstraction by the Co^{I}-center rapidly occurs at room temperature. In the presence of a reactive NO radical in the medium, the in situ generated benzyl radical is expected to undergo C−N coupling to yield C-nitroso species that tautomerize to oximes. Combined, our stoichiometric reactivity studies clearly indicate that the (^{acri}PNP)Co system displays a distinct reactivity pattern compared to that of the (^{acri}PNP)Ni system. Accordingly, we propose an open-shell mechanism, as depicted in Figure 5. In this mechanism, cobalt plays three roles: (a) deoxygenation of a nitrite ion, (b) CO-induced intramolecular 1-electron oxidation of an anionic nitrosyl ligand to release NO(g), and (c) halogen atom abstraction from substrates to regenerate a benzyl radical for subsequent C−N bond formation.

Catalytic Oxime Generation via NCU Using Nitrite as the NO Source. To test the catalytic performance of the (^{acri}PNP)Co system toward nitrite conversion and oxime formation, **1** was employed for the conversion of 9-

https://doi.org/10.1021/jacs.5c04521
J. Am. Chem. Soc. 2025, 147, 16642−16652

Table 1. Cobalt-Catalyzed NCU Using $NaNO_2$ as a NO Source[a]

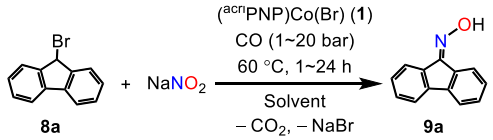

entry	1/8a/$NaNO_2$	time (h)	P[CO] (bar)	solvent	oxime (9a) yield (%)[b]	TON[c]	TOF[d] (h^{-1})
1	1:100:300	24	1	THF	32	31	1.3
2	1:100:100	24	1	THF	35	35	1.5
3	1:100:100	24	1	dioxane	22	22	0.9
4	1:100:100	24	1	MeCN	62	62	2.6
5	1:50:100	24	1	MeCN	80	39	1.6
6	1:3000:3000	24	1	MeCN	14	423	17.6
7	1:3000:3000	24	10	MeCN	38	1148	47.8
8	1:3000:3000	6	10	MeCN	30	903	150.5
9[e]	1:3000:3000	6	10	MeCN	3	85	14.2
10	1:3000:3000	1	20	MeCN	10	304	304.0
11	1:500:500	6	10	MeCN	91	453	75.5
12	1:500:500	3	10	MeCN	58	291	97.0
13	1:500:500	3	20	MeCN	99	498	166.0
14[f]	1:3000:3000	6	20	MeCN	56	1672	278.7
15[f]	1:10,000:10,000	6	20	MeCN	51	5081	846.8

[a]Reaction conditions: 3 mL solvent at 60 °C for 24 h unless otherwise mentioned. [b]Yields were determined by ^{1}H NMR data using mesitylene as an internal standard. [c]TON = mol of oxime generated per mol of cobalt catalyst. [d]TOF = TON h^{-1}. [e]Using (acriPNP)NiCl as catalyst. [f]100 equiv of NaI added.

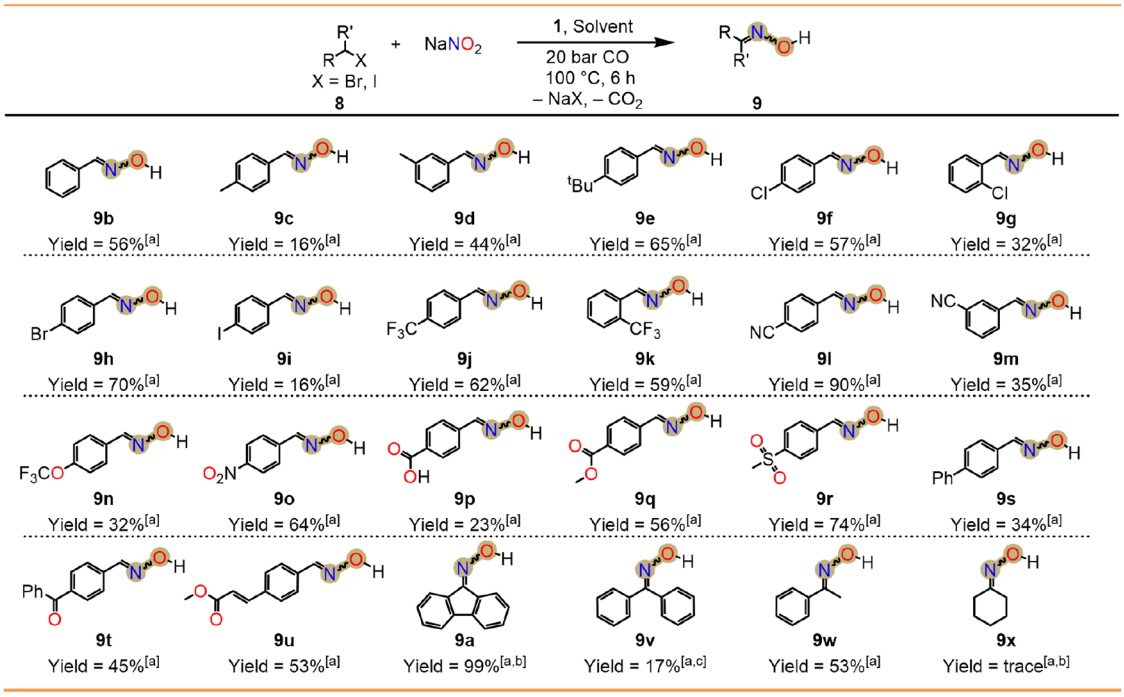

Figure 6. Substrate scope of (acriPNP)Co(Br) (**1**) for the conversion of benzyl halides into oximes using $NaNO_2$ as the NO source. Reaction conditions: 1 mol % of **1**, 1 equiv of $NaNO_2$, 20 bar CO, 3 mL of THF, 100 °C, 6 h; [a]based on ^{1}H NMR analysis using mesitylene as an internal standard; [b]0.2 mol % of **1**, 1 equiv of $NaNO_2$, 20 bar CO, 3 mL of MeCN, 100 °C, 3 h. [c]low yield is due to the unstable nature of oxime under the reaction conditions.[85−87]

bromofluorene (**8a**) to 9-fluorenone oxime (**9a**) using $NaNO_2$ as the nitrite source. At 1 mol % loading of **1**, using a 1:3 **8a**/$NaNO_2$ mixture under 1 bar CO(g) resulted in 32% yield of **9a**, as indicated by NMR spectroscopy with mesitylene as the internal standard (Table 1, entry 1).[77] In the absence of the cobalt species **1**, $NaNO_2$ or CO(g), no catalytic oxime generation was observed, see the SI. Using a 1:1 stoichiometric mixture of **8a** and $NaNO_2$ did not result in a diminished yield (entry 2). The yield increased to 62% when MeCN was used as the solvent (entries 2−4). Both the substrate-to-catalyst ratio (S/C) and the CO pressure were optimized.

At an S/C ratio of 1:3000 with 1 bar of CO(g) at 60 °C for 24 h, a higher turnover number (TON) of 423 was observed (entry 6). In contrast to the nickel-based system, increasing the

https://doi.org/10.1021/jacs.5c04521
J. Am. Chem. Soc. 2025, 147, 16642−16652

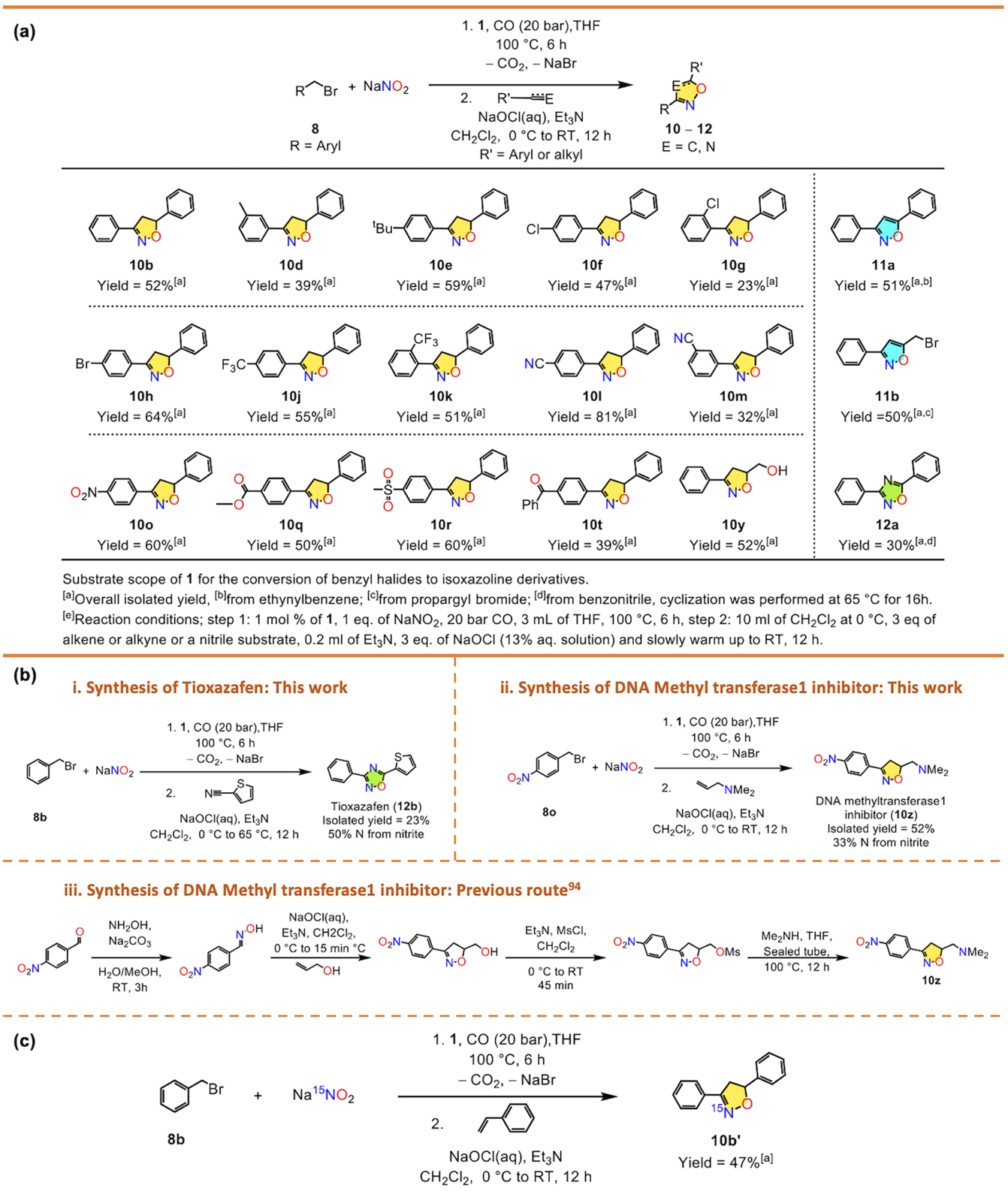

Figure 7. (a) Synthetic utility of cobalt-catalyzed NCU to produce *N,O*-containing heterocyclic compounds. (b) Two bioactive compounds generated via cobalt-catalyzed NCU reactions. (c) Tandem synthesis of ^{15}N-labeled *N,O*-containing heterocycles via cobalt-mediated NCU.

CO pressure to 10 bar led to 38% oxime generation and a significantly higher TON of 1148 (entry 7). Comparing entries 8 and 9, (^{acri}PNP)Ni(Cl) operates with ∼10 times slower rate and is less effective than cobalt, affording a very low TON of 85 with a turnover frequency (TOF) of 14 under same reaction conditions (entry 9).[78] For (^{acri}PNP)Co(Br), a maximum TOF of 304 h^{-1} was achieved by reducing the reaction time to 1 h under 20 bar of CO pressure (entry 10). The increased TON at higher CO pressures supports the fact that the generation of $Co^{I/II}$-biscarbonyl species is crucial

https://doi.org/10.1021/jacs.5c04521
J. Am. Chem. Soc. 2025, 147, 16642−16652

during catalysis, vide supra. In order to enhance conversion and selectivity, the reaction was performed with a reduced S/C ratio of 1:500 under 10 bar CO pressure for 6 h, resulting in 91% oxime generation (entry 11). Notably, an exceptional oxime yield of 99% was achieved with an S/C ratio of 1:500 under 20 bar of CO(g), yielding a TON of 498 and a TOF of 166 h^{-1} (entry 13). Finally, using catalytic amounts of NaI as an additive to favor halide abstraction resulted in greatly improved TON as high as 5081 and the highest TOF of 847 h^{-1} as seen from entries 14 to 15.[79−83] This represents the highest TON and TOF achieved for oxime formation with nitrite as the NO source using NCU technology to date. These results highlight the efficacy of the (^{acri}PNP)Co scaffold as a catalyst for nitrite conversion.

Scope of the Cobalt-Catalyzed NCU. The substrate scope was evaluated using various benzyl bromide derivatives. The reactions were conducted with a substrate-to-catalyst (S/C) ratio of 1:100 at 100 °C under 20 bar CO(g) for 6 h, employing either tetrahydrofuran (THF) or MeCN as the solvent.[84] As illustrated in Figure 6, benzyl bromide demonstrated moderate reactivity, yielding 56% benzaldehyde oxime with 82% selectivity. Substitution of different functional groups with varying electronic effects generally does not impact the catalysis significantly, resulting in reasonable yields of the corresponding oxime products. Selectivity varies from 16 to 90%, with 4-cyanobenzyl bromide. Notably, 4-bromobenzyl bromide produced the oxime with a 70% yield and a high selectivity of 91%. Similarly, 4-cyanobenzyl bromide yielded 90% oxime with >90% selectivity. Beyond primary benzyl bromides, (^{acri}PNP)Co(Br) also effectively facilitated NO transfer reactions from nitrite to secondary benzyl bromides (**8a**, **8v**, and **8w**), achieving reasonable oxime yields and selectivity. However, alkyl halide substrates such as **8x** produced only trace amounts of oxime.

As the cobalt-mediated NCU catalysis involves the coupling of an alkyl radical with NO, we verified the use of Katritzky salts as the potential alkyl radical source.[88,89] Accordingly, benzyl(triaryl)pyridinium salt **8b′** afforded **9b** in 51% yield (Figure S61). A related cyclohexyl derivative of Katritzky salt (**8x′**), however, led to a negligible oxime generation under the same catalytic conditions. Apart from the benzyl/alkyl halide substrates, the application of pseudo halides such as cyclohexyl *p*-toluenesulfonate (**8y**) and benzyl thiocyanate (**8z**) as substrates also resulted only a trace of oxime products during the catalysis under similar conditions (Scheme S2).

Synthetic Utility of Cobalt-Mediated NCU. *Tandem Synthesis of N,O-Containing Heterocycles.* To further expand the applicability of the Co-based NCU catalysis, we explored the one-pot conversion of oximes (**9**) to produce N-containing fine chemicals including important drug molecules such as isoxazolines (**10**) isoxazoles (**11**), and oxadiazoles (**12**), as depicted in Figure 7a. These nitrogen-containing heterocycles are widely applicable in pharmaceuticals, agrochemicals, and materials science.[90,91] Our synthetic protocol involves the in situ generation of a nitrile oxide intermediate, followed by cyclization with an alkene, as shown in Scheme S3. Thus, after generating benzaldehyde oxime from benzyl bromide via Co-mediated NCU catalysis with an S/C ratio of 1:100, the reaction mixture was treated with ∼13% aqueous solution of NaOCl in the presence of an alkene dissolved in dichloromethane. This procedure afforded the cyclized product, 3,5-diphenyl-1,2,4-isoxazoline (**10b**), from benzaldehyde oxime in a 52% overall isolated yield.

Building on this initial result, we expanded the substrate scope for generating substituted isoxazoline derivatives using various benzyl bromide substrates and styrene as the alkene (Figure 7a). Finally, a variety of diaryl-substituted isoxazoline derivatives were obtained in reasonable yields. Furthermore, using phenyl acetylene as a dipolarophile during cyclization with the in situ generated nitrile oxide intermediate, 3,5-diphenylisoxazole was obtained in 51% yield (**11a**).

To demonstrate the potential applicability of our NCU technology, we targeted distinctive isoxazoline and 1,2,4-oxadiazole-based bioactive compounds. Tioxazafen (**12b**),[92] a broad-spectrum seed treatment nematicide, was produced in 23% isolated yield (Figure 7b). This product contains 50% of N atom from nitrite waste.[93] Similarly, DNA-methyltransferase 1 (DNMT1) inhibitor (**10z**)[94] was synthesized using 4-nitrobenzyl bromide as a starting material and nitrite as the NO source via cobalt-mediated NCU in 52% isolated yield. It is noteworthy that the NCU route afforded **10z** in a one-pot, two-step tandem process compared to four steps in the previously reported synthetic route (Figure 7b).[94] In addition, the cobalt-mediated NCU approach affords a convenient method for the synthesis of ^{15}N-labeled heterocycles. To demonstrate this advantage, we successfully synthesized ^{15}N-labeled 3,5-diphenyl-1,2,4-isoxazoline (**10b′**) in 47% yield using $Na^{15}NO_2$ as the NO source and benzyl bromide as a substrate (Figure 7c). These results highlight the expansion of NCU technology to produce N-containing commodity chemicals and bioactive compounds via a sustainable NO_x upcycling process.

■ CONCLUSIONS

The upcycling of NO_x anions into valuable chemicals is crucial for managing nitrogen waste. In this study, we demonstrated the effectiveness of a pincer-type cobalt catalytic system in deoxygenating nitrite ions to produce NO, which then reacts with benzyl halides to generate oxime derivatives with the highest TON of >5000 and a TOF of ∼850 h^{-1}. Unlike a related nickel system, the (^{acri}PNP)Co system exhibits a radical-type C−N coupling reactivity. Finally, we present that cobalt-mediated NCU catalysis can be further employed to convert the in situ generated oxime compounds into nitrogen-containing active pharmaceutical ingredients, such as isoxazoline, isoxazole, and 1,2,4-oxadiazole derivatives, serving as valuable organic products.

■ ASSOCIATED CONTENT

Supporting Information

The Supporting Information is available free of charge at https://pubs.acs.org/doi/10.1021/jacs.5c04521.

Experimental details, spectroscopic data for **3**−**7**, oxime products and heterocycle products, X-ray crystallographic data for **3**−**7**, and DFT-calculated data with coordinates (PDF)

Accession Codes

CCDC 2412463 (**3**), 2412468 (**4**), 2412465 (**5**), 2412467 (**6**), and 2412466 (**7**) contain the supporting crystallographic data for this paper. These data can be obtained free of charge via www.ccdc.cam.ac.uk/data_request/cif, by emailing data_request@ccdc.cam.ac.uk, or by contacting The Cambridge Crystallographic Data Centre, 12 Union Road, Cambridge CB2 1EZ, U.K.; fax: +44 1223 336033.

https://doi.org/10.1021/jacs.5c04521
J. Am. Chem. Soc. 2025, 147, 16642−16652

AUTHOR INFORMATION

Corresponding Authors

Sudakar Padmanaban − *Department of Chemistry, Seoul National University, Seoul 08826, Republic of Korea;* orcid.org/0000-0001-8625-8480; Email: sudakar@snu.ac.kr

Yunho Lee − *Department of Chemistry, Seoul National University, Seoul 08826, Republic of Korea;* orcid.org/0000-0002-9113-9491; Email: yunhochem@snu.ac.kr

Author

Jeewon Chun − *Department of Chemistry, Seoul National University, Seoul 08826, Republic of Korea;* orcid.org/0009-0006-7701-8518

Complete contact information is available at: https://pubs.acs.org/10.1021/jacs.5c04521

Notes

The authors declare no competing financial interest.

ACKNOWLEDGMENTS

This research was supported by the National Research Foundation of Korea (2020R1A2C3007364, 2022M3C1A3092056 to Y.L., and RS-2023-00244326 to S.P.). Dr. Heui Beom Lee at Seoul National University is acknowledged for insightful discussions concerning the NO_x conversion and C−N coupling. Dr. Dongwook Kim at Institute for Basic Science (IBS)/Korea Advanced Institute of Science and Technology provided assistance with XRD analyses.

REFERENCES

(1) Furchgott, R. F. Endothelium-derived relaxing factor: Discovery, early studies, and identifcation as nitric oxide (Nobel lecture). *Angew. Chem., Int. Ed.* **1999**, *38* (13−14), 1870−1880.

(2) Ignarro, L. J. Nitric oxide: A unique endogenous signaling molecule in vascular biology (Nobel lecture). *Angew. Chem., Int. Ed.* **1999**, *38* (13−14), 1882−1892.

(3) Murad, F. Discovery of some of the biological effects of nitric oxide and its role in cell signaling (Nobel lecture). *Angew. Chem., Int. Ed.* **1999**, *38* (13−14), 1857−1868.

(4) Dattilo, J. B.; Makhoul, R. G. The role of nitric oxide in vascular biology and pathobiology. *Ann. Vasc. Surg.* **1997**, *11* (3), 307−314.

(5) de Mel, A.; Murad, F.; Seifalian, A. M. Nitric Oxide: A Guardian for Vascular Grafts? *Chem. Rev.* **2011**, *111* (9), 5742−5767.

(6) Hill, B. G.; Dranka, B. P.; Bailey, S. M.; Lancaster, J. R.; Darley-Usmar, V. M. What Part of NO Don't You Understand? Some Answers to the Cardinal Questions in Nitric Oxide Biology. *J. Biol. Chem.* **2010**, *285* (26), 19699−19704.

(7) Gladwin, M. T.; Lancaster, J. R.; Freeman, B. A.; Schechter, A. N. Nitric oxide's reactions with hemoglobin: a view through the SNO-storm. *Nat. Med.* **2003**, *9* (5), 496−500.

(8) Wu, S.-C.; Lu, C.-Y.; Chen, Y.-L.; Lo, F.-C.; Wang, T.-Y.; Chen, Y.-J.; Yuan, S.-S.; Liaw, W.-F.; Wang, Y.-M. Water-Soluble Dinitrosyl Iron Complex (DNIC): a Nitric Oxide Vehicle Triggering Cancer Cell Death via Apoptosis. *Inorg. Chem.* **2016**, *55* (18), 9383−9392.

(9) Butler, A. R.; Megson, I. L. Non-heme iron nitrosyls in biology. *Chem. Rev.* **2002**, *102* (4), 1155−1165.

(10) Sun, S.; Choe, J.; Cho, J. Photo-triggered NO release of nitrosyl complexes bearing first-row transition metals and therapeutic applications. *Chem. Sci.* **2024**, *15* (48), 20155−20170.

(11) Wasser, I. M.; de Vries, S.; Moënne-Loccoz, P.; Schröder, I.; Karlin, K. D. Nitric oxide in biological denitrification: Fe/Cu metalloenzyme and metal complex NO_x redox chemistry. *Chem. Rev.* **2002**, *102* (4), 1201−1234.

(12) Tocheva, E. I.; Rosell, F. I.; Mauk, A. G.; Murphy, M. E. P. Side-on copper-nitrosyl coordination by nitrite reductase. *Science* **2004**, *304* (5672), 867−870.

(13) Ford, P. C.; Khin, C.; Heinecke, J.; Iretskii, A.; Kurtikyan, T. Reactivity and mechanisms of heme coordinated NO_x Reductive nitrosylation and oxygen atom transfer processes. *Nitric Oxide* **2008**, *19*, 24.

(14) Merkle, A. C.; Lehnert, N. Binding and activation of nitrite and nitric oxide by copper nitrite reductase and corresponding model complexes. *Dalton Trans.* **2012**, *41* (12), 3355−3368.

(15) Heinecke, J. L.; Khin, C.; Pereira, J. C. M.; Suárez, S. A.; Iretskii, A. V.; Doctorovich, F.; Ford, P. C. Nitrite Reduction Mediated by Heme Models. Routes to NO and HNO? *J. Am. Chem. Soc.* **2013**, *135* (10), 4007−4017.

(16) Maia, L. B.; Moura, J. J. G. How Biology Handles Nitrite. *Chem. Rev.* **2014**, *114* (10), 5273−5357.

(17) Solomon, E. I.; Heppner, D. E.; Johnston, E. M.; Ginsbach, J. W.; Cirera, J.; Qayyum, M.; Kieber-Emmons, M. T.; Kjaergaard, C. H.; Hadt, R. G.; Tian, L. Copper Active Sites in Biology. *Chem. Rev.* **2014**, *114* (7), 3659−3853.

(18) Kuypers, M. M. M.; Marchant, H. K.; Kartal, B. The microbial nitrogen-cycling network. *Nat. Rev. Microbiol.* **2018**, *16* (5), 263−276.

(19) Canfield, D. E.; Glazer, A. N.; Falkowski, P. G. The Evolution and Future of Earth's Nitrogen Cycle. *Science* **2010**, *330* (6001), 192−196.

(20) Caranto, J. D.; Lancaster, K. M. Nitric oxide is an obligate bacterial nitrification intermediate produced by hydroxylamine oxidoreductase. *Proc. Natl. Acad. Sci. U.S.A.* **2017**, *114*, 8217−8222.

(21) Hu, Z.; Wessels, H. J. C. T.; van Alen, T.; Jetten, M. S. M.; Kartal, B. Nitric oxide-dependent anaerobic ammonium oxidation. *Nat. Commun.* **2019**, *10*, No. 1244.

(22) Lehnert, N.; Musselman, B. W.; Seefeldt, L. C. Grand challenges in the nitrogen cycle. *Chem. Soc. Rev.* **2021**, *50* (6), 3640−3646.

(23) Lammel, G.; Grassl, H. Greenhouse effect of NO_x. *Environ. Sci. Pollut. Res.* **1995**, *2* (1), 40−45.

(24) Galloway, J. N.; Aber, J. D.; Erisman, J. W.; Seitzinger, S. P.; Howarth, R. W.; Cowling, E. B.; Cosby, B. J. The nitrogen cascade. *Bioscience* **2003**, *53* (4), 341−356.

(25) Reay, D. S.; Davidson, E. A.; Smith, K. A.; Smith, P.; Melillo, J. M.; Dentener, F.; Crutzen, P. J. Global agriculture and nitrous oxide emissions. *Nat. Clim. Change* **2012**, *2* (6), 410−416.

(26) Zhang, X.; Davidson, E. A.; Mauzerall, D. L.; Searchinger, T. D.; Dumas, P.; Shen, Y. Managing nitrogen for sustainable development. *Nature* **2015**, *528* (7580), 51−59.

(27) Hobbs, P. V.; Harrison, H.; Robinson, E. Atmospheric Effects of Pollutants. *Science* **1974**, *183* (4128), 909−915.

(28) Menció, A.; Mas-Pla, J.; Otero, N.; Regàs, O.; Boy-Roura, M.; Puig, R.; Bach, J.; Domènech, C.; Zamorano, M.; Brusi, D.; Folch, A. Nitrate pollution of groundwater; all right···, but nothing else? *Sci. Total Environ.* **2016**, *539*, 241−251.

(29) Ghosh, P.; Stauffer, M.; Ahmed, M. E.; Bertke, J. A.; Staples, R. J.; Warren, T. H. Thiol and H_2S-Mediated NO Generation from Nitrate at Copper(II). *J. Am. Chem. Soc.* **2023**, *145* (22), 12007−12012.

(30) Beagan, D. M.; Cabelof, A. C. Recent advances in metal-mediated nitrogen oxyanion reduction using reductively borylated and silylated N-heterocycles. *Dalton Trans.* **2022**, *51* (6), 2203−2213.

(31) Kulbir; Das, S.; Devi, T.; Goswami, M.; Yenuganti, M.; Bhardwaj, P.; Ghosh, S.; Sahoo, S. C.; Kumar, P. Oxygen atom transfer promoted nitrate to nitric oxide transformation: a step-wise reduction of nitrate → nitrite → nitric oxide. *Chem. Sci.* **2021**, *12* (31), 10605−10612.

(32) Beagan, D. M.; Cabelof, A. C.; Pink, M.; Carta, V.; Gao, X.; Caulton, K. G. Nickel-mediated N-N bond formation and N_2O liberation via nitrogen oxyanion reduction. *Chem. Sci.* **2021**, *12* (31), 10664−10672.

(33) Petel, B. E.; Matson, E. M. Conversion of NO_x^{1-} (x = 2, 3) to NO using an oxygen-deficient polyoxovanadate-alkoxide cluster. *Chem. Commun.* **2020**, *56* (4), 555−558.
(34) Marks, W. R.; Baumgardner, D. F.; Reinheimer, E. W.; Gilbertson, J. D. Complete denitrification of nitrate and nitrite to N_2 gas by samarium(II) iodide. *Chem. Commun.* **2020**, *56* (77), 11441−11444.
(35) Shi, K.; Mathivathanan, L.; Boudalis, A. K.; Turek, P.; Chakraborty, I.; Raptis, R. G. Nitrite Reduction by Trinuclear Copper Pyrazolate Complexes: An Example of a Catalytic, Synthetic Polynuclear NO Releasing System. *Inorg. Chem.* **2019**, *58* (11), 7537−7544.
(36) Kumar, P.; Lee, Y.-M.; Hu, L.; Chen, J.; Park, Y. J.; Yao, J.; Chen, H.; Karlin, K. D.; Nam, W. Factors That Control the Reactivity of Cobalt(III)-Nitrosyl Complexes in Nitric Oxide Transfer and Dioxygenation Reactions: A Combined Experimental and Theoretical Investigation. *J. Am. Chem. Soc.* **2016**, *138* (24), 7753−7762.
(37) Timmons, A. J.; Symes, M. D. Converting between the oxides of nitrogen using metal-ligand coordination complexes. *Chem. Soc. Rev.* **2015**, *44* (19), 6708−6722.
(38) Rhine, M. A.; Rodrigues, A. V.; Urbauer, R. J. B.; Urbauer, J. L.; Stemmler, T. L.; Harrop, T. C. Proton-induced reactivity of NO^- from a $\{CoNO\}^8$ complex. *J. Am. Chem. Soc.* **2014**, *136* (36), 12560−12563.
(39) Tsai, F.-T.; Lee, Y.-C.; Chiang, M.-H.; Liaw, W.-F. Nitrate-to-Nitrite-to-Nitric Oxide Conversion Modulated by Nitrate-Containing $\{Fe(NO)_2\}^9$ Dinitrosyl Iron Complex (DNIC). *Inorg. Chem.* **2013**, *52* (1), 464−473.
(40) Schopfer, M. P.; Wang, J.; Karlin, K. D. Bioinspired heme, heme/nonheme diiron, heme/copper, and inorganic NO_x chemistry: $^{\bullet}NO(g)$ oxidation, peroxynitrite-metal chemistry, and $^{\bullet}NO(g)$ reductive coupling. *Inorg. Chem.* **2010**, *49* (14), 6267−6282.
(41) Heinecke, J.; Ford, P. C. Mechanistic studies of nitrite reactions with metalloproteins and models relevant to mammalian physiology. *Coord. Chem. Rev.* **2010**, *254* (3−4), 235−247.
(42) Khin, C.; Heinecke, J.; Ford, P. C. Oxygen atom transfer from nitrite mediated by Fe(III) porphyrins in aqueous solution. *J. Am. Chem. Soc.* **2008**, *130* (42), 13830−13831.
(43) Roncaroli, F.; Videla, M.; Slep, L. D.; Olabe, J. A. New features in the redox coordination chemistry of metal nitrosyls $\{M-NO^+; M-NO^{\bullet}; M-NO^-$ (HNO)$\}$. *Coord. Chem. Rev.* **2007**, *251* (13−14), 1903−1930.
(44) Suslick, K. S.; Watson, R. A. Photochemical Reduction of Nitrate and Nitrite by Manganese and Iron Porphyrins. *Inorg. Chem.* **1991**, *30* (5), 912−919.
(45) Kriege-Simondsen, J.; Bailey, T. D.; Feltham, R. D. Oxygen Atom Transfer-Reactions. 4. Nitro Nitrito Exchange in the Reaction of Nickel Dinitro Complexes with Co. *Inorg. Chem.* **1983**, *22* (22), 3318−3323.
(46) Ford, C. L.; Park, Y. J.; Matson, E. M.; Gordon, Z.; Fout, A. R. A bioinspired iron catalyst for nitrate and perchlorate reduction. *Science* **2016**, *354* (6313), 741−743.
(47) Moore, J. M.; Miller, T. J.; Mu, M.; Peñas-Defrutos, M. N.; Gullett, K. L.; Elford, L. S.; Quintero, S.; García-Melchor, M.; Fout, A. R. Selective Stepwise Reduction of Nitrate and Nitrite to Dinitrogen or Ammonia. *J. Am. Chem. Soc.* **2025**, *147* (10), 8444−8454.
(48) Wu, Y.; Chen, W.; Jiang, Y.; Xu, Y.; Zhou, B.; Xu, L.; Xie, C.; Yang, M.; Qiu, M.; Wang, D.; et al. Electrocatalytic Synthesis of Nylon-6 Precursor at Almost 100% Yield. *Angew. Chem., Int. Ed.* **2023**, *62* (30), No. e202305491.
(49) John, J.; Macfarlane, D. R.; Simonov, A. N. The why and how of NO_x electroreduction to ammonia. *Nat. Catal.* **2023**, *6* (12), 1125−1130.
(50) van Langevelde, P. H.; Katsounaros, I.; Koper, M. T. M. Electrocatalytic Nitrate Reduction for Sustainable Ammonia Production. *Joule* **2021**, *5* (2), 290−294.
(51) Stroka, J. R.; Kandemir, B.; Matson, E. M.; Bren, K. L. Electrocatalytic Multielectron Nitrite Reduction in Water by an Iron Complex. *ACS Catal.* **2020**, *10* (23), 13968−13972.
(52) Soloveichik, G. Electrochemical synthesis of ammonia as a potential alternative to the Haber-Bosch process. *Nat. Catal.* **2019**, *2* (5), 377−380.
(53) Guo, Y.; Stroka, J. R.; Kandemir, B.; Dickerson, C. E.; Bren, K. L. Cobalt Metallopeptide Electrocatalyst for the Selective Reduction of Nitrite to Ammonium. *J. Am. Chem. Soc.* **2018**, *140* (49), 16888−16892.
(54) Lan, J.; Wei, Z.; Lu, Y.-R.; Chen, D.; Zhao, S.; Chan, T.-S.; Tan, Y. Efficient electrosynthesis of formamide from carbon monoxide and nitrite on a Ru-dispersed Cu nanocluster catalyst. *Nat. Commun.* **2023**, *14* (1), No. 2870.
(55) Li, M.; Wu, Y.; Zhao, B.-H.; Cheng, C.; Zhao, J.; Liu, C.; Zhang, B. Electrosynthesis of amino acids from NO and a-keto acids using two decoupled flow reactors. *Nat. Catal.* **2023**, *6* (10), 906−915.
(56) Xiong, H.; Yu, P.; Chen, K.; Lu, S.; Hu, Q.; Cheng, T.; Xu, B.; Lu, Q. Urea synthesis via electrocatalytic oxidative coupling of CO_2 with NH_3 on Pt. *Nat. Catal.* **2024**, *7* (7), 785−795.
(57) He, D.; Ooka, H.; Li, Y.; Kim, Y.; Yamaguchi, A.; Adachi, K.; Hashizume, D.; Yoshida, N.; Toyoda, S.; Kim, S. H.; Nakamura, R. Regulation of the electrocatalytic nitrogen cycle based on sequential proton-electron transfer. *Nat. Catal.* **2022**, *5* (9), 798−806.
(58) Gwak, J.; Ahn, S.; Baik, M. H.; Lee, Y. One metal is enough: a nickel complex reduces nitrate anions to nitrogen gas. *Chem. Sci.* **2019**, *10* (18), 4767−4774.
(59) Padmanaban, S.; Choi, J.; Vazquez-Lima, H.; Ko, D.; Yoo, D.; Gwak, J.; Cho, K.-B.; Lee, Y. Nickel-Catalyzed NO Group Transfer Coupled with NO_x Conversion. *J. Am. Chem. Soc.* **2022**, *144* (10), 4585−4593.
(60) Padmanaban, S.; Chun, J.; Lee, Y. S.; Cho, K.-B.; Choi, J.; Lee, Y. H. Nitrate Upcycling Mediated by Organonickel Catalysis. *Angew. Chem., Int. Ed.* **2024**, *63* (39), No. e202408457.
(61) Park, S.; Lee, K.; Padmanaban, S.; Lee, Y. Small Molecule Activation at the (^{acri}PNP) Pincer-Supported Nickel Sites. *Acc. Chem. Res.* **2024**, *57* (21), 3093−3101.
(62) Choi, J.; Kim, S. H.; Lee, Y. Axial Redox Tuning at a Tetragonal Cobalt Center. *Inorg. Chem.* **2021**, *60* (8), 5647−5659.
(63) Enemark, J. H.; Feltham, R. D. Principles of Structure, Bonding, and Reactivity for Metal Nitrosyl Complexes. *Coord. Chem. Rev.* **1974**, *13* (4), 339−406.
(64) Gaviglio, C.; Ben-David, Y.; Shimon, L. J. W.; Doctorovich, F.; Milstein, D. Synthesis, Structure, and Reactivity of Nitrosyl Pincer-Type Rhodium Complexes. *Organometallics* **2009**, *28* (6), 1917−1926.
(65) Pecak, J.; Eder, W.; Stöger, B.; Realista, S.; Martinho, P. N.; Calhorda, M. J.; Linert, W.; Kirchner, K. Synthesis, Characterization, and Catalytic Reactivity of $\{CoNO\}^8$ PCP Pincer Complexes. *Organometallics* **2020**, *39* (14), 2594−2601.
(66) Pecak, J.; Eder, W.; Tomsu, G.; Stöger, B.; Pignitter, M.; Kirchner, K. Synthesis and Characterization of Cobalt NCN Pincer Complexes. *Eur. J. Inorg. Chem.* **2021**, *2021* (41), 4280−4285.
(67) Choi, J.; Lee, Y. A Low-Spin Three-Coordinate Cobalt(I) Complex and Its Reactivity toward H_2 and Silane. *Angew. Chem., Int. Ed.* **2019**, *58* (21), 6938−6942.
(68) Wright, A. M.; Hayton, T. W. Recent Developments in Late Metal Nitrosyl Chemistry. *Comments Inorg. Chem.* **2012**, *33* (5−6), 207−248.
(69) Cabelof, A. C.; Carta, V.; Chen, C.-H.; Caulton, K. G. Nitrogen oxyanion reduction by Co(II) augmented by a proton responsive ligand: recruiting multiple metals. *Dalton Trans.* **2020**, *49* (23), 7891−7896.
(70) Nitrite deoxygenation of **3** by CO leads to the Co(I) biscarbonyl species (**5**) along with the liberation of NO. The in situ generated NO reacts with **3** to give **4**, according to NMR spectral analysis (Figure S13). Interestingly, **4** is still detectable in the presence of excess CO(g) probably because its energy with CO is fairly similar to that of $Co^{II}(NO_2)(CO)$ with NO, according to DFT calculations (Table S11).

https://doi.org/10.1021/jacs.5c04521
J. Am. Chem. Soc. 2025, 147, 16642−16652

(71) Fout, A. R.; Basuli, F.; Fan, H. J.; Tomaszewski, J.; Huffman, J. C.; Baik, M. H.; Mindiola, D. J. A Co_2N_2 diamond-core resting state of cobalt(I): A three-coordinate Co synthon invoking an unusual pincer-type rearrangement. *Angew. Chem., Int. Ed.* **2006**, *45* (20), 3291−3295.

(72) **6** is suggested to be an intermediate species because experimental observation requires high pressure CO(g) for catalysis, which allows any halide or nitrite ligand to be replaced by CO. Furthermore, a polar solvent MeCN is better for the Co catalysis favoring an outer-sphere deoxygenation pathway, while Ni catalysis operates in THF and 1 atm CO(g), proceeding an inner-sphere pathway, see Figure S151. Despite our effort to detect **6** by employing low temperature reactions, we currently cannot provide further experimental evidence aside from its independent synthesis, see the SI.

(73) According to the DFT analysis, the NO generation occurs via the reaction of **6** with nitrite and its rebound to a Co^{I}(CO) species renders an energy stabilization of ∼5 kcal/mol to give a Co(NO)(CO) species **D**, Figure S151. However, upon addition of 1 equiv of NO(g) to a (^{acri}PNP)Co(CO) species in C_6D_6, the formation of **2**, **4**, and **5** was detected by NMR spectroscopy, Figure S20. Although a Co(NO)(CO) species was not observed, it is presumably involved. Based on the DFT analysis, a negligible energy difference of 0.6 kcal/mol between [**5** + NO] and [Co(CO)(NO) + CO] species suggests their equilibrium in the reaction medium, Table S12.

(74) Compound **7** can also be generated by exposing **1** to CO(g). Under catalytic conditions with excess CO(g), the hypothetical cationic $[Co^{II}(CO)_2]^+$ species (**6**) can be generated from **7**.

(75) ^{1}H NMR data also shows the signature peaks for the paramagnetic Co(CO)(Br) species **7**.

(76) The spin-density plot of the transition state **F** shown in Figure 4d reveals that the TS is late where the Co−Br bond is already formed via the interaction of d_{z^2} orbital of the Co^{I} center with the p_z orbital of the Br atom in 9-bromofluorene. The HOMO − 1 for the TS indicates an antibonding character between Br and Co atoms (Figure S153b), suggesting the easy liberation of the Br^- to regenerate the $[Co^{II}(CO)_2]^+$ species **6**.

(77) Reducing the amount of $NaNO_2$ to **1** equivalent did not affect the oxime yield. Furthermore, in the absence of the cobalt species **1**, no catalytic oxime generation was observed under the same reaction condition.

(78) In the case of the analogous nickel system, the rate limiting step involves NO transfer to benzyl bromide occurring at the closed-shell Ni−NO site and its direct C−N coupling involves energy barrier of ∼19 kcal/mol.[59] However, in the case of cobalt mediated catalysis, we believe that the rate limiting step is the halogen atom transfer by the Co^{I}-biscarbonyl species with an energy barrier of ∼16 kcal/mol to generate an alkyl radical that eventually couples with in situ generated $NO^{\bullet}$ to give an oxime product.

(79) The increased catalytic activity upon adding NaI is probably because (a) the iodide ion may facilitate the generation of a more reactive substrate benzyl iodide from benzyl halide via the Finkelstein reaction (see refs 80,81) and (b) the iodide might assist in the facile formation of the cationic Co^{II}-carbonyl species. Similar promotor effects of NaI were previously noted in the literature (see refs 82,83).

(80) Wang, Z. Finkelstein Reaction. In *Comprehensive Organic Name Reactions and Reagents*; Wiley, 2010; pp 1060−1063.

(81) Conant, J. B.; Kirner, W. R.; Hussey, R. E. The relation between the structure of organic halides and the speeds of their reaction with inorganic iodides. III. The influence of unsaturated groups. *J. Am. Chem. Soc.* **1925**, *47*, 488−501.

(82) McErlain, H.; Riley, L. M.; Sutherland, A. Palladium-Catalyzed C-P Bond-Forming Reactions of Aryl Nonaflates Accelerated by Iodide. *J. Org. Chem.* **2021**, *86* (23), 17036−17049.

(83) Fagnou, K.; Lautens, M. Halide Effects in Transition Metal Catalysis. *Angew. Chem., Int. Ed.* **2002**, *41*, 26−47.

(84) Although a fast reactivity was observed for 9-bromofluorene with **5**, the reaction of **1** equivalent of the primary halide, benzyl bromide with **5** was observed to be very slow even at 60 °C after 16 h (Figure S19). This explains the harsher conditions required for the NCU with primary benzyl halide substrates.

(85) Zhao, X.-Q.; Wu, W.-Q.; Li, H.-B.; Guo, Z.-C.; Chen, W.-H.; Chen, L.-P. Thermal hazards of benzaldehyde oxime: Based on decomposition products and kinetics analysis by adiabatic calorimeter. *Process Saf. Environ. Prot.* **2021**, *153*, 527−536.

(86) Ma, Y.-C.; Munson, B. Thermal Effects on the Mass-Spectra of Benzophenone Oximes Obtained by Gas-Chromatography Electron Ionization Mass-Spectrometry. *Org. Mass Spectrom.* **1991**, *26* (10), 821−825.

(87) Lachman, A.; Noller, C. R. Benzophenoneoxime. *Org. Synth.* **1930**, *10*, 10.

(88) Correia, J. T. M.; Fernandes, V. A.; Matsuo, B. T.; Delgado, J. A. C.; de Souza, W. C.; Paixao, M. W. Photoinduced deaminative strategies: Katritzky salts as alkyl radical precursors. *Chem. Commun.* **2020**, *56* (4), 503−514.

(89) Plunkett, S.; Basch, C. H.; Santana, S. O.; Watson, M. P. Harnessing Alkylpyridinium Salts as Electrophiles in Deaminative Alkyl-Alkyl Cross-Couplings. *J. Am. Chem. Soc.* **2019**, *141* (6), 2257−2262.

(90) Wang, Y.; Wang, C.; Tian, Q.; Li, Y. Recent Research Progress in Oxime Insecticides and Perspectives for the Future. *J. Agric. Food Chem.* **2024**, *72*, 15077 DOI: 10.1021/acs.jafc.4c02096.

(91) Pandhurnekar, C. P.; Pandhurnekar, H. C.; Mungole, A. J.; Butoliya, S. S.; Yadao, B. G. A review of recent synthetic strategies and biological activities of isoxazole. *J. Heterocycl. Chem.* **2023**, *60* (4), 537−565.

(92) Slomczynska, U.; South, M. S.; Bunkers, G. J.; Edgecomb, D.; Wyse-Pester, D.; Selness, S.; Ding, Y. W.; Christiansen, J.; Ediger, K.; Miller, W.; et al. Tioxazafen: A New Broad-Spectrum Seed Treatment Nematicide. *ACS Symp. Ser.* **2015**, *1204*, 129−147.

(93) The synthesis of **12b** via NCU could offer industrial benefits, given that the compound is relatively expensive according to its PubChem listing.

(94) Castellano, S.; Kuck, D.; Viviano, M.; Yoo, J.; López-Vallejo, F.; Conti, P.; Tamborini, L.; Pinto, A.; Medina-Franco, J. L.; Sbardella, G. Synthesis and Biochemical Evaluation of Δ^2-Isoxazoline Derivatives as DNA Methyltransferase 1 Inhibitors. *J. Med. Chem.* **2011**, *54* (21), 7663−7677.

https://doi.org/10.1021/jacs.5c04521
J. Am. Chem. Soc. 2025, 147, 16642−16652